Chapter 17

Thermoelectric Power Generation Optimization by Thermal Design Means

Patricia Aranguren and David Astrain

Additional information is available at the end of the chapter

http://dx.doi.org/10.5772/65849

Abstract

One of the biggest challenges of the twenty-first century is to satisfy the demand for electrical energy in an environmentally speaking clean way. Thus, it is very important to search for new alternative energy sources along with increasing the efficiency of current processes. Thermoelectric power generation, by means of harvesting waste heat and converting it into electricity, can help to achieve above-mentioned goal. Nowadays, efficiency of thermoelectric power generators limits them to become key technology in electric power generation, but their performance has potential of being optimized, if thermal design of such generators is optimized. Heat exchangers located on both sides of thermoelectric modules (TEMs), mass flow of refrigerants and occupancy ratio (the area covered by TEMs related to base area), among others, need to be fine-tuned in order to obtain the maximum net power generation (thermoelectric power generation minus consumption of auxiliary equipment). Finned dissipator, cold plate, heat pipe and thermosiphon are experimentally tested to maximize net thermoelectric generation on real-working furnace based on computational model. Maximum generation of 137 MWh/year using thermosiphons is achieved with 32% of area covered by TEMs.

Keywords: thermoelectric generator, optimization, computational model, heat exchanger, occupancy ratio

1. Introduction

The excessive use of fossil fuels has lead into severe environmental issues. Consequently, global warming, greenhouse gases emissions, climate change, acid rain and ozone depletion are commonly heard on the media. Moreover, combustible resources are limited, and more

restrict environmental regulations are arising. Hence, one of the biggest challenges of the twenty-first century is to satisfy energetic demand in environmentally friendly manner.

In order to fulfill the previous aim, new tendencies are springing, such as smart utilization of energy throughout boosting savings, avoiding waste and developing more efficient, so as less fuel consuming, equipment and through the development of renewable energies. Thermoelectric generation contributes to diminish the impact that fossil fuels generate. A better exploitation of fossil fuels is possible due to their potential to harvest waste heat and convert it into electricity, improving efficiency of energy generating systems.

Nowadays, thermoelectrics is an emerging technology, which converts waste heat into electricity. Solid-state operation of thermoelectric generators (TEGs) eliminates the presence of moving parts and/or chemical reactions, and thus the maintenance is reduced to minimum. It cancels greenhouse gases emissions to environment, and long lives are achieved due to safe operation of thermoelectric generators.

Waste heat is defined as by-product heat of a process, which is not exploited afterward, but it is emitted to the ambient. Nowadays, great amount of produced energy is lavished as waste heat, and at least 40% of the primary energy utilized in industrialized countries is emitted to the ambient as waste heat [1]. Nevertheless, most of this waste heat presents low temperature levels (low temperature grade heat), as **Figure 1** presents, explaining the most studied use up to the moment, heating of fluids for heating or other purposes [2–4]. It has been estimated, that double the heating needs of the United States, the 16.4 % of the primary energy consumed worldwide, could be supplied with waste heat [1].

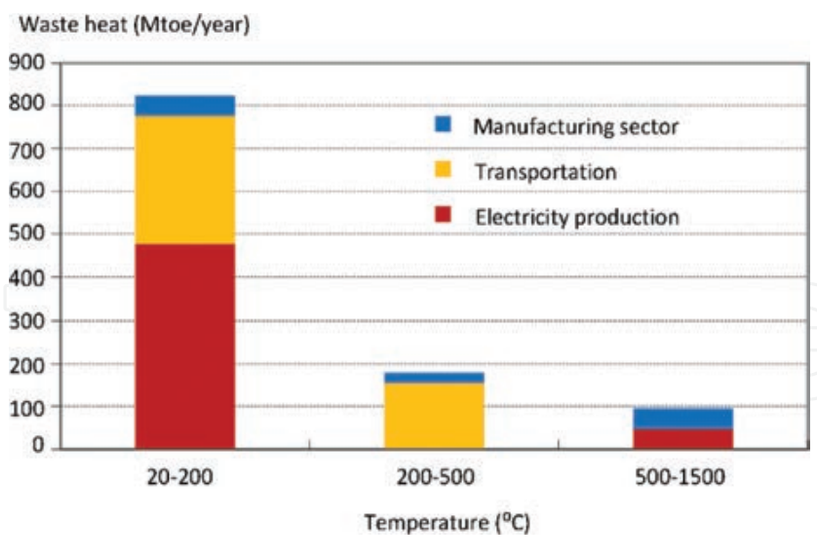

Figure 1. Temperature grade of waste heat [1].

Particular temperature grade, that waste heat presents, restricts applicable technologies to harvest it with effective conversion to electricity. However, thermoelectricity is a promising technology to recover low temperature grade waste heat [5]. Several studies have ratified promising future, that TEGs demonstrate ability to produce electric energy from waste heat

http://dx.doi.org/10.5772/65849

of different applications. Some of them are introduced here: Bi_2Te_3-PbTe TEG obtains 211 kW electrical power from waste heat of Portland Cement Rotary Kilns [6]; study conducted in Japan presents potential of recovering radiant heat from steelmaking processes with 10-kW-class grid-connected TEG system [7]; thermoelectric power density of approximately 193.1 W/m^2 is obtained from waste heat of biomass gasifier [8], while power density nearly 100 W/m^2 is obtained from combustion chamber [9]; thermoelectric generator integrated within photovoltaic/thermal absorber improves total efficiency of generating system [10]; nearly 5 kWh/year-m^2 can be produced from solar ponds [11]; and the most common and studied TEGs, which recover waste heat from exhaust gas of vehicles in order to improve their efficiency [12–14].

Efficiency, that normally TEGs present between 5 and 10% [15, 16], is deterrent to make these systems attractive enough to pass the thin line between laboratory experimentation and simulation and commercialization and expansion of this technology. Nowadays, the two issues that are the main objectives are to improve efficiency of thermoelectric generation systems: the first objective is development and improvement of thermoelectric materials through modification of conventional materials with new technologies, such as introducing nanostructures into conventional semiconductors [17, 18] or creating novel thermoelectric materials, such as polymers [19], oxides [20], half-heusler [21] or skutterudites [22]; the second objective is to optimize thermal design of the system. To achieve the latter objective, different approaches can be studied and implemented, for example, heat exchangers located on both sides of thermoelectric modules can be optimized through many different approaches that will be detailed afterwards, and also the number of thermoelectric modules (TEMs) has to be properly selected to reach the maximum thermoelectric generation. Occupancy ratio δ, parameter that includes number of used TEMs M_{TEM}, that is, ratio between area covered by TEMs A_{TEM} and base area A_b of heat exchangers (Eq. (1)), is crucial parameter to optimize thermoelectric generation:

$$\delta = \frac{M_{TEM} A_{TEM}}{A_b}. \tag{1}$$

Although it seems, that higher number of thermoelectric modules would mean higher thermoelectric power generation, thermal resistance per thermoelectric module of heat exchangers worsens, if occupancy ratio rises, resulting in reduction in thermoelectric power generation per TEM. Each application presents optimum point, where thermoelectric power generation is maximum [23–25]. Moreover, reduction in the number of modules does not only imply increase in thermoelectric power generation, but also decrease in initial investment.

Optimization of heat exchangers attached to hot and cold sides of TEMs is very important to maximize thermoelectric power generation, and improvement in thermal resistances will result in higher temperature difference between hot and cold TEM sides close to temperature difference between heat exchangers, and, hence, will provide higher thermoelectric power generation [26–29]. Optimization of heat dissipation systems can be done by modifying their geometry, such as increasing number, height or spacing of fins of finned dissipator [30, 31] or by properly selecting channel's diameter, internal distribution and/or internal inserts of cold

plates [32–35]. Besides, inclusion of novel heat exchangers, such as heat pipes [23, 36] or thermosiphons [37–39], could procure higher thermoelectric power generation. Nevertheless, increase in power generation does not necessarily mean improvement in net generation (usable energy obtained from any application) due to increase in the consumption of auxiliary equipment, coolant pump or fans, in order to optimize the thermal behavior of the systems [9, 33, 34, 40].

In this chapter, computational optimization of real furnace located in Spain is performed giving experimental data of thermal resistances of different kinds of heat exchangers (finned dissipator, cold plate, heat pipe and thermosiphon) as function of occupancy ratio, mass flow of refrigerants and heat power to dissipate. Net power generation, that is, thermoelectric power generation minus power consumption of auxiliary equipment Eq. (2), is computed and maximized by means of previously mentioned parameters:

$$\dot{W}_{net} = \dot{W}_{TEM} - \dot{W}_{aux}. \tag{2}$$

2. Computational methodology

Thermoelectric generators produce electricity when there is temperature gradient between hot and cold sides of TEM. Therefore, harvesting of waste heat to produce electricity by thermoelectric generation is becoming very interesting field of studying. Gratuity of waste heat and its great presence in numerous applications overcome low efficiency values, that TEGs present; however, until to date not many applications have been materialized. Initial investment and payback time (due to low efficiency) are deterrents for the development of this technology. This is the reason why computational models are playing very important role in the development of thermoelectric power generation. Due to complicated physical phenomena, that take place in TEGs, knowledge of TEG-based systems' behavior in different conditions is crucial to evaluate their potential, as well as to improve their performance, basing on both thermoelectric material properties and properties and dimensions of heat exchangers located on both sides of TEMs.

Modeling of each component of TEG is essential to perform accurate simulation of behavior of TEG-based systems. TEG is formed by TEMs (which present thermoelectric material, ceramic plates, joints…), the heat exchangers that are located on both sides of thermoelectric modules, as well as by any elementary component for correct assembly of the whole system; consequently, everything needs to be included into the model [41, 42]. Moreover, each thermoelectric phenomenon (Seebeck effect, Thomson effect, Peltier effect and Joule effect) needs to be taken into account, especially in thermoelectric generation due to significant temperature difference between hot and cold sides of TEMs, to obtain accurate results [43–45]; likewise, thermoelectric properties need to be defined as function of temperature not to commit big errors [46]. Furthermore, resolution has to bear in mind transient state of operation [47, 48], especially if trying to model combustion systems with permanent changes in per-

http://dx.doi.org/10.5772/65849

formance and, thus, permanent changes in temperature and mass flow, as vehicles or combustion stoves. The latest applications are very precious due to gratuity of waste heat.

Computational model developed to optimize any thermoelectric application, especially TEGs, which harvest waste heat to produce electricity, includes each thermoelectric phenomenon, each component of the system, temperature dependence of thermoelectric properties and transient state of operation. Moreover, it includes novel parameters, such as occupancy ratio, that is, the ratio between area covered by thermoelectric modules and dissipative base area (Eq. (1)), mass flow of refrigerants and temperature decrease in flue gases when flowing along TEG. Previously mentioned parameters are determinant of net thermoelectric power generation (Eq. (2)), the main parameter to optimize in any application.

Computational methodology uses finite differences approach to solve behavior of the system. It solves each thermoelectric phenomenon, Seebeck effect Eq. (3), Peltier effect Eq. (4), Thomson effect Eq. (5) and Joule effect Eq. (6), and it includes Fourier law of heat conduction used in one-dimensional form, when heat power generation Eq. (7) takes place:

$$\alpha_{AB} = \frac{dE_t}{dT} = \alpha_A - \alpha_B, \tag{3}$$

$$\dot{Q}_{Peltier} = \pm \pi_{AB} I = \pm IT(\alpha_A - \alpha_B), \tag{4}$$

$$\dot{Q}_{Thomson} = -\sigma \vec{I}(\overrightarrow{\Delta T}), \tag{5}$$

$$\dot{Q}_{Joule} = R_0 I^2, \tag{6}$$

$$\rho c_p \frac{\delta T}{\delta t} = k\left(\frac{\delta^2 T}{\delta x_2}\right) + \overline{q}. \tag{7}$$

Resolution methodology is based on previously published and validated computational model [26, 49].

Temperature decrease in flue gases is achieved by discretizing pipe, where flue gases circulate. Within each block, thermoelectric phenomenon is solved. To that objective, temperature of flue gases must be known. Temperature of heat source in each block T_H^i is selected as the mean temperature between entry T_e^i and exit T_s^i temperatures of each block, $T_H^i = T_m^i = \frac{1}{2}\left(T_e^i + T_s^i\right)$. Exit temperature is obtained using heat power extracted from flue gases by TEG in that block, Eq. (8). As blocks are located sequentially, exit temperature of previous block coincides with entry temperature of the following block, $T_e^{i+1} = T_s^i$:

$$T_s^i = T_e^i - \frac{\dot{Q}^i}{\dot{m}_{gas} c_p}. \tag{8}$$

Figure 2 presents block "i" of pipe and discretization of that block in order to apply finite differences method to solve thermoelectric phenomena. There are totally 16 nodes, which represent the whole TEG: node 1 is heat source, while node 16 is heat sink; nodes 2 and 15 are hot side and cold side heat exchangers, respectively; and nodes 3–14 represent TEM, where nodes 3 and 14 are hot and cold sides and from node 4 to node 13 thermoelectric material is represented. Electrical analogy is composed by thermal resistances, thermal capacities and absorbed or generated heat fluxes. R_{HD}^i and R_{CD}^i stand for resistances of hot side and cold side heat dissipators, respectively, R_{cont}^i are contact resistances and R_{per}^i and R_{tor}^i stand for two alternative ways for heat power to reach heat sink. The best scenario would be where the total amount of heat power circulates through thermoelectric modules, but in real application there are parasitic heats that circulate along other elements. In this case, heat power that reaches cold sink directly from hot source is born in mind through R_{per}^i, and heat power that flows through assembling screws attaching cold and hot dissipators is represented by R_{tor}^i.

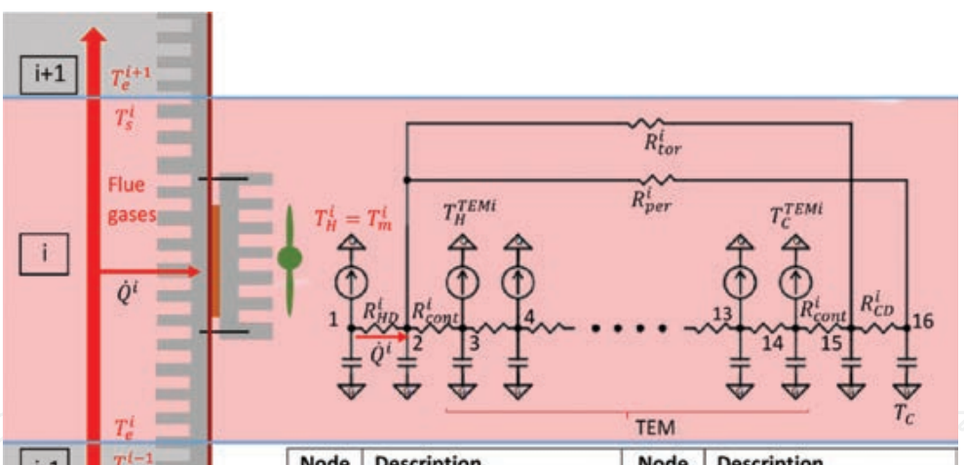

Node	Description	Node	Description
1	Heat source	14	Cold side of the TEM
2	Hot side heat dissipator	15	Cold side heat dissipator
3	Hot side of the TEM	16	Heat sink
4-13	Thermoelectric material		

Figure 2. Thermoelectric generator discretization of block "i".

Particularly, this model considers temperature loss of flue gases, while they circulate along TEG, occupancy ratio and mass flow of refrigerants. Methodology used can be seen in **Figure 3**. The first step is to choose the number of blocks, in which the pipe is discretized, n_{blo}. Once this parameter is selected and information of application is introduced into the model, resolution starts from the first block, where the mean temperature of the block is

http://dx.doi.org/10.5772/65849

supposed to be entry temperature of the block, in the case of first block's temperature is that of flue gases. The next step is to suppose heat power that needs to be dissipated by heat exchangers, $\dot{Q}_i^c$, parameter that determines thermal resistance of dissipation systems, as it will be seen in the next section. Thermal resistances of dissipation systems are now determined, so the finite differences method can be used to solve thermoelectric phenomena, obtaining heat power to dissipate and closing the most interior iteration loop. As heat dissipators are function of heat power to dissipate, and at the same time, they define amount of heat that TEG is extracting from flue gases, this issue is solved through an iteration process, which obtains the heat power to dissipate. Once known, the mean temperature of the block needs to be obtained. The mean temperature is computed as the mean value between entry and exit temperatures of flue gases, and exit temperature is obtained using Eq. (8), so new iteration loop solves this situation. Finally, when everything has converged, thermoelectric generation is saved and resolution follows to the next block. This procedure keeps on until each block has been solved and the total power generation has been computed. **Figure 3** presents schematic of the methodology used to obtain thermoelectric power generation.

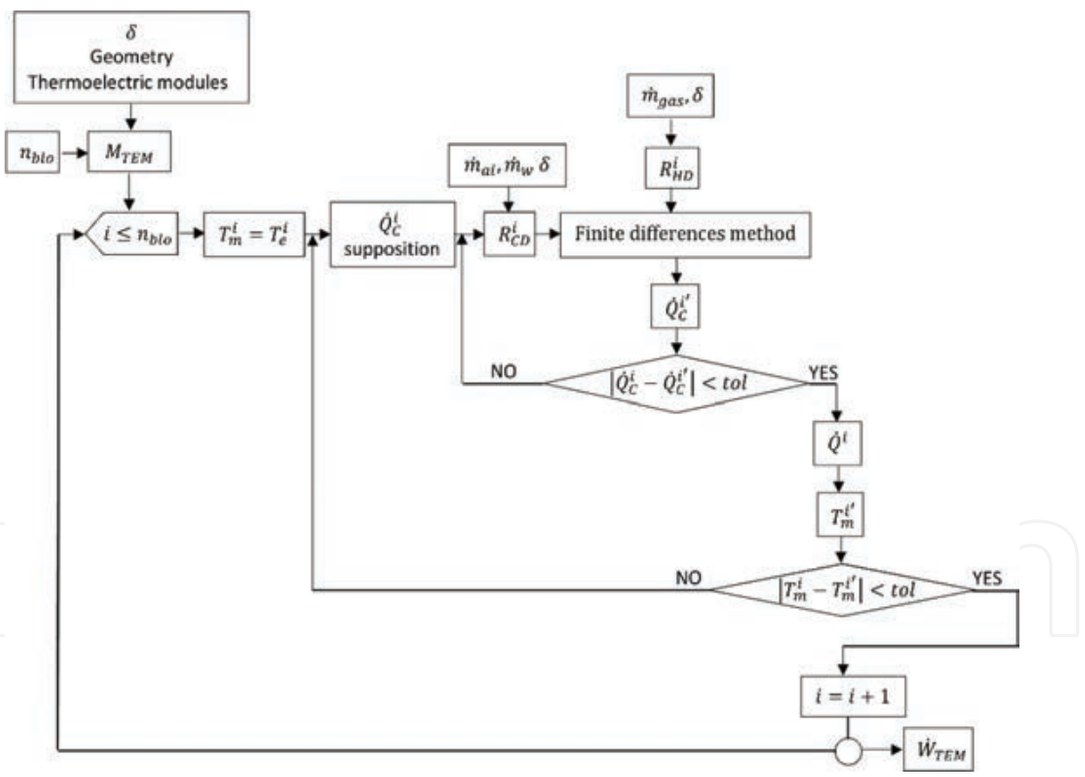

Figure 3. Computational model for thermoelectric power generation.

Net power generation, Eq. (2), is afterward obtained, giving power consumption of auxiliary equipment, determined by the test conducted to thermally characterize the different types of heat exchangers studied, finned dissipator, cold plate, heat pipe and thermosiphon. Experimental thermal characterization of these systems is explained in the next section, very

important data that are essential to include into the computational model in order to calculate accurate results about thermoelectric power generation from any application.

3. Thermal characterization of heat exchangers

Thermal characterization of heat dissipation systems is crucial to obtain accurate results using computational model presented in the above section. Four different heat dissipation systems (cold plate, finned dissipator, heat pipe and thermosiphon) have been experimentally tested in order to obtain their thermal resistances as function of influential parameters in thermoelectric power generation: occupancy ratio, mass flow of refrigerants and heat power to dissipate.

Thermal resistances are presented as thermal resistances per thermoelectric module and computed through experimentation as Eq. (9) presents:

$$R^{TEM} = \frac{T_m^{HX} - T_{amb}}{\frac{\dot{Q}_C}{M_{TEM}}}. \tag{9}$$

T_m^{HX} stands for average temperature of each heat exchanger, where heat is applied and T_{amb} represents ambient temperature, it is selected constant, 22°C, as heat dissipation systems are placed into climatic chamber ensuring constant temperature during experiments. To test different occupancy ratios, heat plates of the same size of TEMs have been used. Heat power to dissipate corresponds to electric power supplied to heat plates ($\dot{Q}_C = V_{HP} I_{HP}$). One side of heat plate is thermally isolated to assure that total supplied electrical power is transformed into heat power directed to heat exchangers. Finally, the number of TEMs (M_{TEM}) contributes to get medium thermal resistance per thermoelectric module of each heat exchanger.

Variable parameters during experiments are occupancy ratio, heat power to dissipate and mass flow of the refrigerants. Each configuration has been replicated three times ($M_{sample} = 3$) to reduce the random standard uncertainty of the mean ($S_{\bar{R}^{TEM}}$). Expanded uncertainty of measured resistances (Eq. (10)) is composed of previously mentioned uncertainty (Eqs. (11) and (12)), systematic standard uncertainty (Eq. (13)) and level of confidence, in this case chosen to be the 95% [50]:

$$U_{R^{TEM}} = 2\left(b_{R^{TEM}}^2 + s_{\bar{R}^{TEM}}^2\right)^{\frac{1}{2}}, \tag{10}$$

http://dx.doi.org/10.5772/65849

$$s^2_{\bar{R}^{TEM}} = \frac{1}{M_{sample}\left(M_{sample}-1\right)} \sum_{k=1}^{M_{sample}} (R_k^{TEM} - \bar{R}^{TEM})^2, \tag{11}$$

$$\bar{R}^{TEM} = \frac{1}{M_{sample}} \sum_{k=1}^{M_{sample}} R_k^{TEM}, \tag{12}$$

$$b^2_{R^{TEM}} = \left(\frac{\partial R^{TEM}}{\partial T_m^{HX}}\right)^2 b^2_{T_m} + \left(\frac{\partial R^{TEM}}{\partial T_{amb}}\right)^2 b^2_{T_{amb}} + \left(\frac{\partial R^{TEM}}{\partial V_{HP}}\right)^2 b^2_{V_{HP}} + \left(\frac{\partial R^{TEM}}{\partial I_{HP}}\right)^2 b^2_{I_{HP}}. \tag{13}$$

3.1. Cold plate

Use of fluids as heat carrier enhances thermal transfer. In the case of tested system, water has been used in order to characterize heat dissipation system thermally and to analyze results, if net thermoelectric generation increases. Heat dissipation system is formed by cold plate (cold side heat exchanger), fan-coil composed by core and fans to make air circulate through its fins (the secondary heat exchanger in charge of reducing temperature of heat carrier fluid), pump, necessary elements to direct fluid flow and secure safe performance of dissipation system and sensors to obtain the data, as shown in **Figure 4** [51]. Cold plate has 26 transversal channels with diameter 6.2 mm and two manifolds to distribute water coolant along the channels. Plate exterior dimensions are 190 mm × 230 mm. The fan-coil presents core formed by two 8 mm diameter pipes with total number of 12 passes. It is provided with wind tunnel, which presents three fans to make air circulate through its fins. Pump used in the system has been specially chosen, and pumping level can be chosen from one to four using switch.

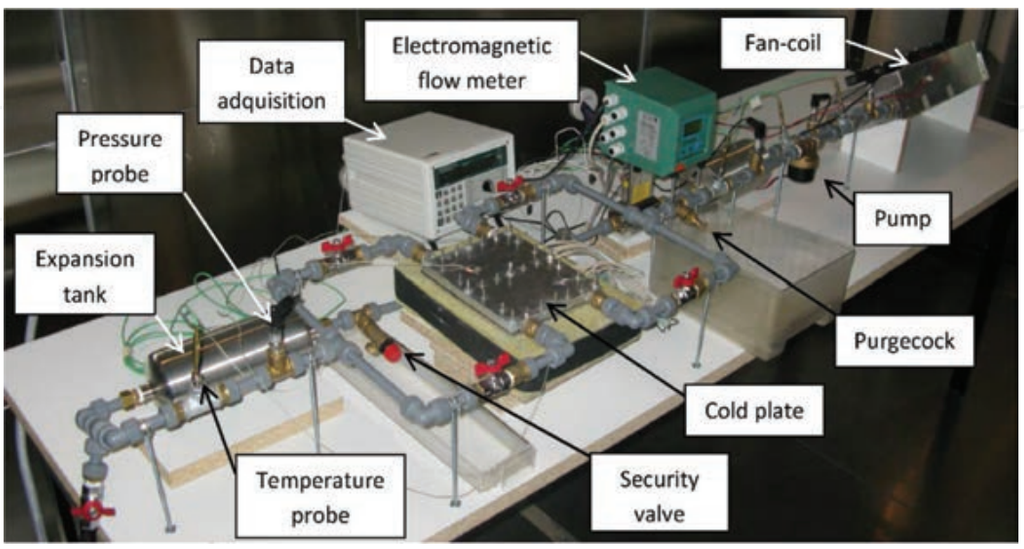

Figure 4. Test bench used to obtain experimentally thermal resistance of cold plate system [51].

Power consumption of pump and fans of fan-coil as function of water and air mass flows, respectively, is shown in **Figure 8**, which represents all relations between mass flows and consumption of auxiliary equipment used for different heat exchangers.

Thermal characterization has been performed using experimental data and validated computational model, enabling to obtain thermal resistances on test bench. Description of the model and validation details can be found in publications, Aranguren et al. [40, 51]. Thermal resistance of cold plate is not function of heat power to dissipate due to small influence of this parameter on temperature of water coolant, the term that could influence on thermal resistance. **Figure 5a** depicts influence of heat power for specific water mass flow. **Figure 5b** presents the influence of occupancy ratio on thermal resistance per thermoelectric module for fixed heat power and water mass flow. As ratio grows, implying that number of TEMs grows, thermal resistance worsens due to the reduction in dissipative area per thermoelectric module. **Figure 5c** presents dependence of thermal resistance air and water mass flows at different occupancy ratio. Occupancy ratio has a great influence on thermal resistance, showing that increasing number of modules harms thermal resistance. Within the same occupancy ratio, water and air mass flow show influence on thermal resistance, most notable for high occupancy ratios, where dissipative area is reduced and any improvement in convective coefficients procures important benefits to thermal resistance.

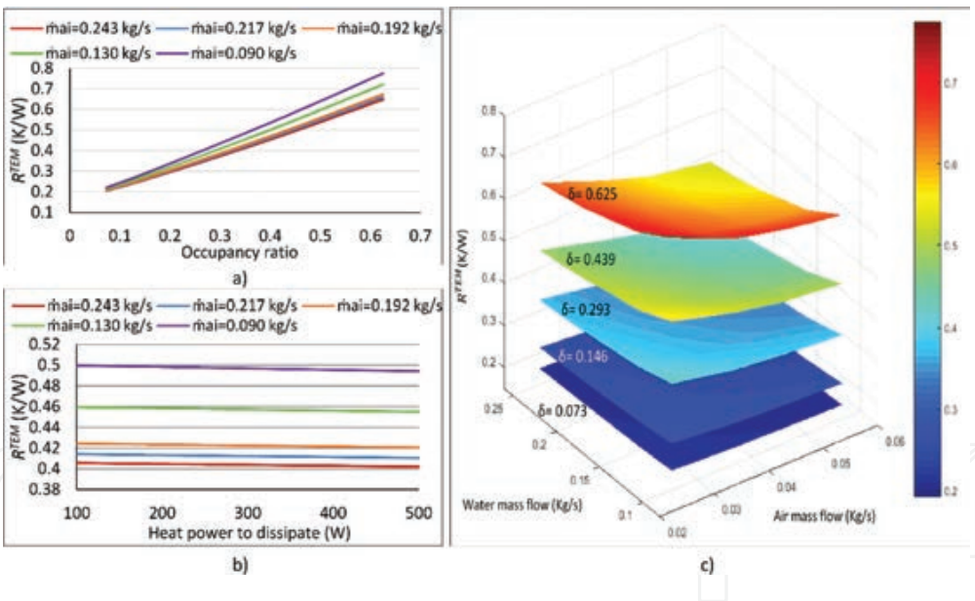

Figure 5. Thermal resistance per thermoelectric module of cold plate. (a) Thermal resistance as function of heat power to dissipate for $\dot{m}_w = 0.055\ \mathrm{kg/s}$, (b) thermal resistance as function of occupancy ratio for $\dot{m}_w = 0.044\ \mathrm{kg/s}$, (c) thermal resistance as function of air and water mass flows.

3.2. Finned dissipator

Finned dissipators up to date have been the most used heat exchangers in thermoelectricity due to their simplicity. Studied finned dissipator has external dimensions of 190 mm × 230 mm, base thickness of 14.5 mm and height, thickness and spacing of fins of 39.5, 1.5 and 3.3 mm,

http://dx.doi.org/10.5772/65849

respectively. It is provided with wind tunnel, which includes two fans to make air circulate along its fins. The finned dissipator is shown in **Figure 7a**. Relation between power consumption of fans and air mass flow is presented in **Figure 8**.

Figure 6 presents thermal resistance of finned dissipator as function of heat power to dissipate, occupancy ratio and mass flow of air. Heat power to dissipate does not determine thermal resistance, as (shown in **Figure 6a** and **b**). Each panel of **Figure 6** presents thermal resistance of finned dissipator as function of heat power to dissipate, the first one for fixed air mass flow of $\dot{m}_{ai} = 0.024$ kg/s and the second one for $\dot{m}_{ai} = 0.060$ kg/s. Occupancy ratio influences highly thermal resistance, and higher occupancy ratios procure higher thermal resistances per thermoelectric module, due to the reduction in dissipative area per TEM, as presented in **Figure 6**. **Figure 6d** shows the influence of air mass flow, and for high occupancy ratios, influence is more remarkable than for low ones, due to the higher benefits that improvement in convection coefficients has for small convective areas.

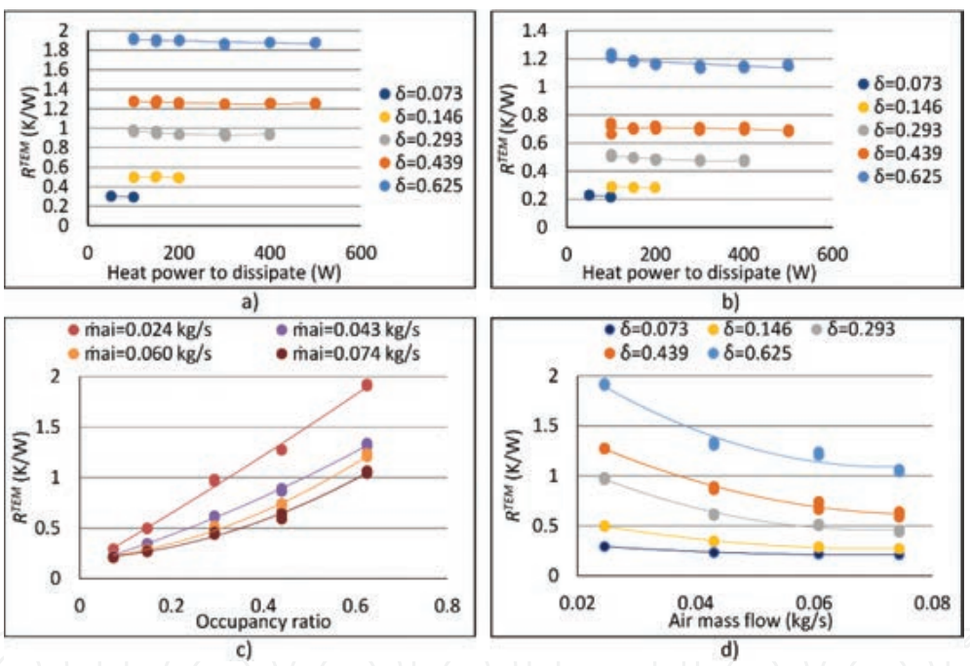

Figure 6. Thermal resistance per thermoelectric module of finned dissipator. (a) Thermal resistance as function of heat power to dissipate for $\dot{m}_{ai} = 0.024$ kg/s, (b) thermal resistance as function of heat power to dissipate for $\dot{m}_{ai} = 0.060$ kg/s, (c) thermal resistance as function of occupancy ratio, (d) thermal resistance as function of air mass flow.

The expanded uncertainty of thermal resistance R^{TEM} is equal to ±10.80%.

3.3. Heat pipe

Heat pipes are passive devices able to transfer great amount of heat with small temperature differences. Heat pipes present sealed volumes provided with porous media and divided into

three regions: evaporator, where heat is absorbed; condenser, where heat is emitted; and adiabatic region. Working fluid evaporates due to heat gained and flows into the condenser, where it condensates and returns to evaporator due to capillary lift. Tested heat pipe is composed by 10 8 mm diameter pipes with length of 350 mm and spaced 7 mm. Base external dimension of heat pipe is 90 × 192.5 mm^2, and pipes are inserted, being the region, where heat arrives. To help condensation of working fluid water, heat pipe includes wind tunnel provided with fan, as **Figure 7b** presents. Air mass flow as function of power consumption is shown in **Figure 8**.

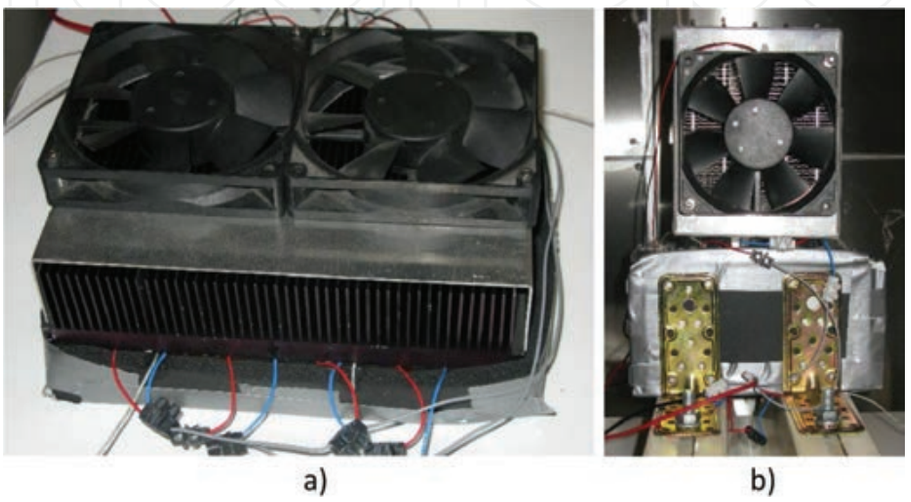

Figure 7. Heat exchanger devices: (a) Finned dissipator; (b) heat pipe.

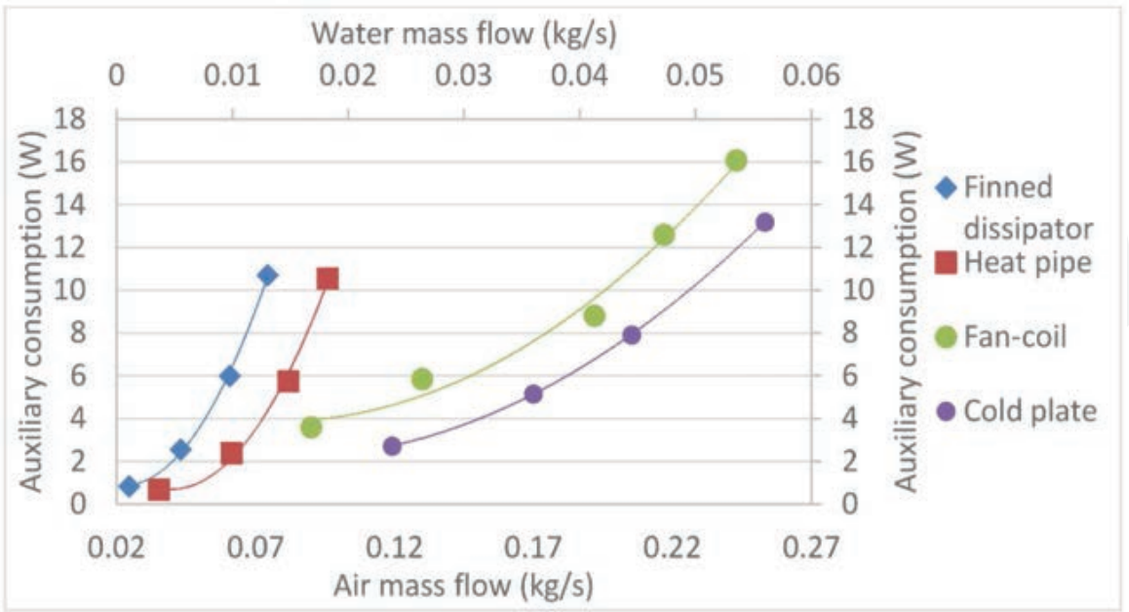

Figure 8. Power consumption of fans of finned dissipator, heat pipe and fan-coil as function of air mass flow and power consumption of the pump of cold plate heat dissipation system as function of water mass flow.

http://dx.doi.org/10.5772/65849

Thermal resistance of heat pipe is function of heat power to dissipate. Condensation and boiling coefficients depend on temperature of fluid and walls, and, therefore, thermal resistance is function of heat power that has to be dissipated, as shown **Figure 9a**. Occupancy ratio and air mass flow present the same tendency as in previous cases, as shown in **Figure 9b**, **c** and **d**. The expanded uncertainty of thermal resistance R^{TEM} is equal to ±7.88%.

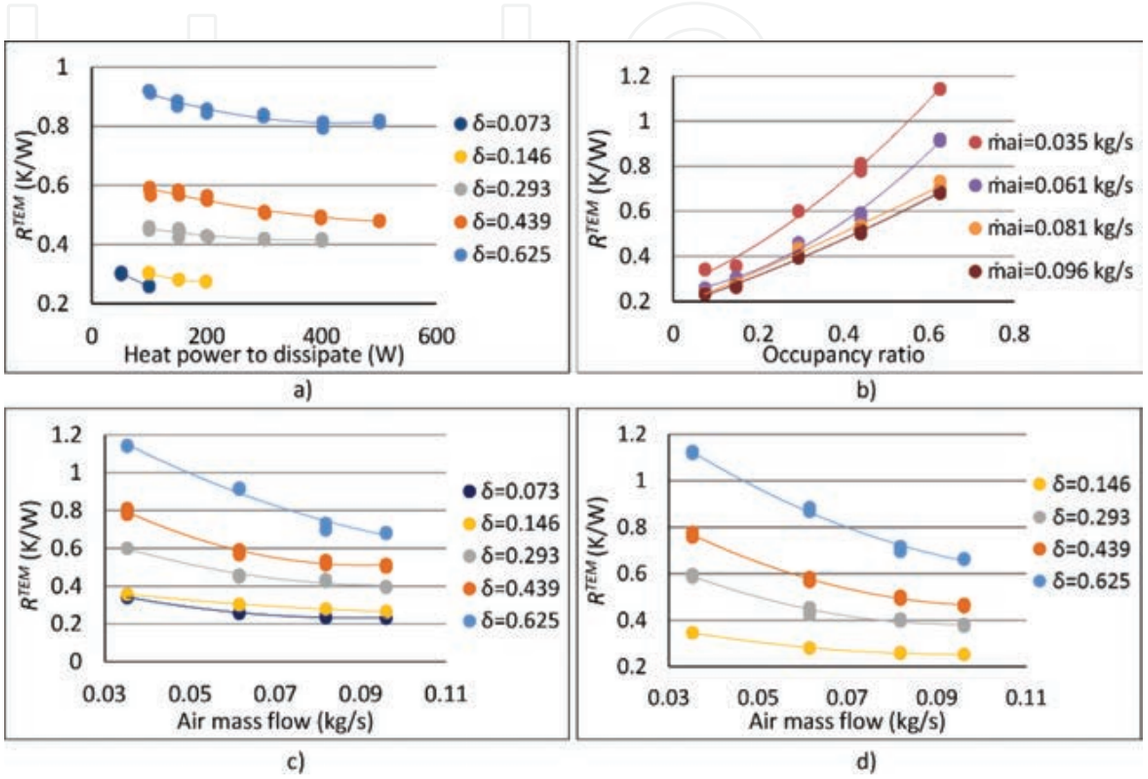

Figure 9. Thermal resistance per thermoelectric module of heat pipe. (a) Thermal resistance as function of heat power to dissipate for $\dot{m}_{ai} = 0.061\ \text{kg/s}$, (b) thermal resistance as function of occupancy ratio for $\dot{Q}_C = 100\ \text{W}$, (c) thermal resistance as function of air mass flow for $\dot{Q}_C = 100\ \text{W}$, and (d) thermal resistance as function of air mass flow for $\dot{Q}_C = 150\ \text{W}$.

3.4. Thermosiphon

Thermosiphons with phase change present the same physical phenomena, than heat pipes, but they do not present porous media. Hence, they need gravitational forces to ensure that condensate heat carrier returns to evaporator. Tested thermosiphon has vessel of 160 × 200 mm^2 and 22 mm diameter pipe that connects the circuit. Pipe is divided into six channels with diameter of 10 mm. Condenser area is composed by seven levels extended along 850 mm with width of 240 mm and depth of 500 mm. This area has 8 mm spaced fins in order to help working fluid, R134a, to condensate. Thermosiphon does not present auxiliary equipment as previous heat exchangers presented. **Figure 10** shows heat dissipation system. Thermosiphon test does not present any fans to help working fluid to condensate, so thermal resistance depends only on heat power to dissipate and occupancy ratio, as displayed in **Figure 11**. Due to natural

convection to exterior space and boiling and condensation coefficients, thermal resistance depends on calorific power to a higher extent to dissipate. Higher heat power to dissipate procures higher temperatures, which benefit transfer coefficients involved, and procuring lower thermal resistances, especially high occupancy ratios, is more affected due to high occupation, as presented in **Figure 11b**. The expanded uncertainty of thermal resistance R^{TEM} is equal to ±8.42%.

Figure 10. Tested thermosiphon.

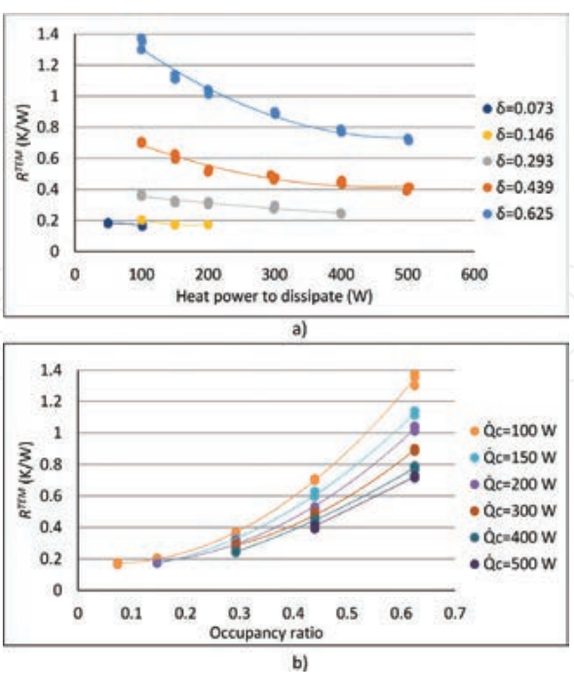

Figure 11. Thermal resistance per thermoelectric module of thermosiphon. (a) Thermal resistance as function of heat power to dissipate, (b) thermal resistance as function of occupancy ratio.

http://dx.doi.org/10.5772/65849

4. Thermoelectric computational optimization of waste heat energy harvesting from real application

Computational model, which enables determining behavior of any TEG and thermal characterization of four different types of studied heat exchangers used to optimize net thermoelectric power generation of real application, is tested on furnace located in Spain. Computational model computes thermoelectric power generation, including calculation power consumption of auxiliary equipment shown in **Figure 8**, and net power generation can be computed (Eq. 2) as well, which is a real target of optimization in any application.

Selected application is furnace, which works 24 h a day, 350 days a year. Temperature of flue gases is 187°C and mass flow is 5.49 kg/s. Chimney has diameter of 0.8 m, transversal area of 0.5 m^2 and height of 12 m. Therefore, available surface to locate TEG is 33.6 m^2. Flue gases emitted to ambient atmosphere are heat source of TEG, while ambient air is heat sink. Temperature of heat sink has been chosen as medium temperature of the year of the location of the furnace, T_{amb} = 17 °C. TEMs simulated are TG12-8-01L from Marlow Industries [52], where hot and cold sides area equals to 40 × 40 mm^2 and TEMs can work up to 250°C on hot side.

Optimization is done for cold side of TEG, where four types of heat exchangers are simulated as function of occupancy ratio and mass flow of refrigerants in order to look for the maximum net power generation. On hot side, that is, interior of chimney, finned dissipator with base thickness of 4 mm and height, thickness and spacing of fins of 50, 6 and 1.5 mm, respectively, have been simulated. Thermal resistance of the latter heat exchanger has been computed as function of occupancy ratio and velocity of flue gases using a Computational Fluid Dynamics program, ANSYS Fluent. Eq. (14) presents thermal resistance of hot side of TEG per thermoelectric module:

$$R^{TEM} = 0.046127 - 0.887591\delta - 0.000251 v_{gas} + 0.385376/\ln(v_{gas}) + 0.304593\delta^2 - 0.281665/\ln^2(v_{gas}) + 4.35262\delta/\ln(v_{gas}), \quad (14)$$

Total consumption of auxiliary equipment is essential to obtain net thermoelectric power generation, the goal of this optimization. Consumption of auxiliary equipment is obtained as function of mass flow presented in **Figure 8** and with accounting for number of TEM units necessary to cover the whole available surface of the chimney, totally 769 units. Cold plate, finned dissipator and heat pipe present auxiliary consumption, while thermosyphon does not, as explained in previous section. As it can be seen in **Figures 5**, **6** and **9**, increment in mass flow of refrigerants, with simultaneous increment in auxiliary equipment consumption, causes improvement in thermal resistances. This fact leads to higher thermoelectric power generation, due to improvement in heat transfer on both sides of the TEMs, obtaining higher difference of temperature between their sides and consequently higher thermoelectric power generation. Nevertheless, consumption of auxiliary equipment grows, so it is not so clear as in the case, when increasing mass flow of refrigerants leads to increase in net power generation. **Figure 12**

shows thermoelectric and net power generation as function of occupancy ratio, when finned dissipators are located on cold side of TEG. It can be seen, that higher air mass flow produces higher thermoelectric power generation; however, net power generation has optimum near the second smallest mass flow simulated, and after this value, net power generation decreases significantly, even obtaining negative values for small occupancy ratios and high mass flow of the air.

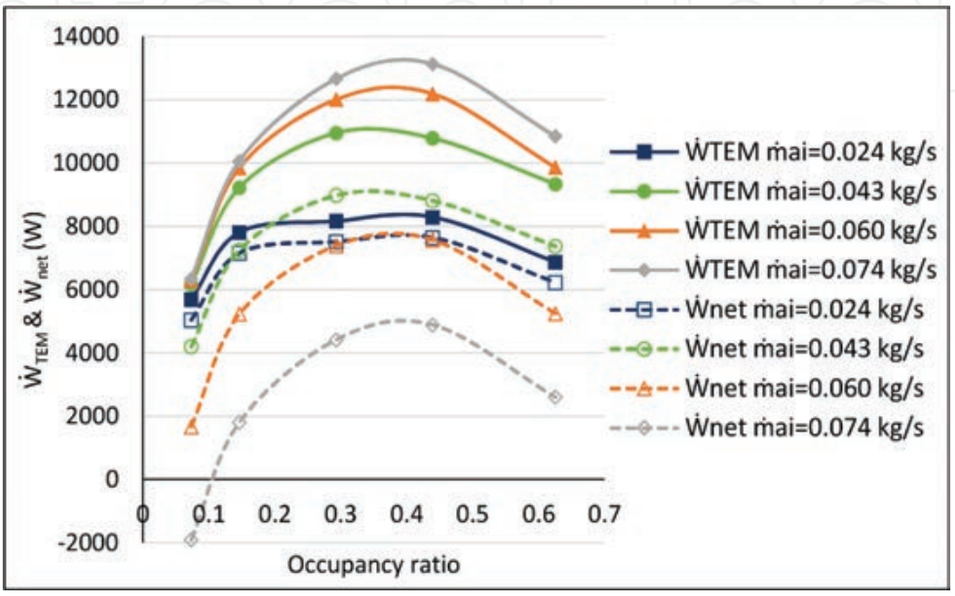

Figure 12. Thermoelectric and net power generation as function of occupancy ratio, when finned dissipators are simulated on cold side of the chimney.

Occupancy ratio is also determined for thermoelectric power generation. Higher occupancy ratio leads to higher thermal resistances per thermoelectric module and, therefore, less power generation per module unit; however, number of units to produce electricity is higher. Once more, it is necessary to elaborate optimization to get the maximum net power generation point. **Figure 12** presents the influence of this parameter, when finned dissipators are simulated on cold side. Occupation ratio value that provides maximum power generation is equal to $\delta \approx 0.4$, that is, optimum is reached, when approximately 40% of available surface is covered by TEMs only. This optimization is crucial to obtain the highest thermoelectric power generation and to optimize initial investment as well, because reduction in number of TEMs, which is necessary to install, reduces the cost of the application.

Figure 13 presents optimum points for net power generation for each occupancy ratio simulated. These points have been obtained by optimizing mass flow of refrigerants of every heat exchanger at each value of occupancy ratio. **Figure 13** shows that the best cold side heat exchanger for this case is thermosiphon, obtaining up to 16280 W from waste heat of the furnace. The optimum occupancy ratio that provides this value equals to $\delta = 0.32$. The number of TEMs necessary to cover 32% of chimney surface is 6720, and the smallest TEMs number is required, if compared with other optimum values as function of occupancy ratio. Therefore,

http://dx.doi.org/10.5772/65849

thermosiphons are heat exchangers that not only provide the highest net thermoelectric power generation, but also the ones that require the smallest initial investment. Moreover, these systems have no moving parts, so they are completely robust and lack of maintenance.

Thermosiphons produce 30% more net optimal power than the second best option, heat pipes. Besides, occupancy ratio to maximize net power generation for heat pipes is higher, $\delta \approx 0.42$, so the initial investment has to be approximately 30% higher to obtain the maximum electrical energy. If optimal heat exchangers are compared with cold plates and finned dissipators, electrical energy production is 72 and 86% higher. Cold plates present optimum values of δ higher than thermosiphons, while finned dissipators present approximately the same occupancy ratio, so the same initial investment. Consumption of auxiliary equipment is deterrent, and small thermal resistances that cold plate presents produce higher thermoelectric power generation, but large consumption of auxiliary equipment negatively influences on net power generation, as **Figure 13** shows, even when auxiliary equipment consumption has been optimized to obtain the maximum net power generation for each occupancy ratio.

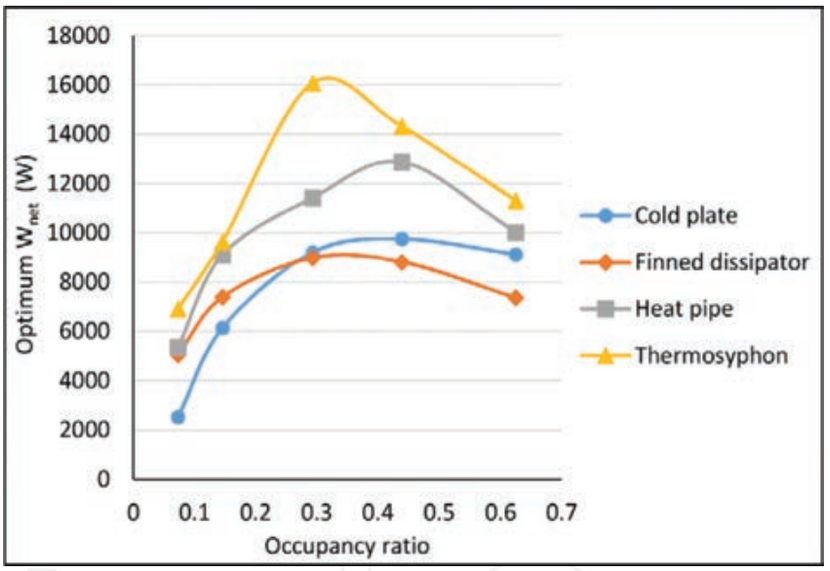

Figure 13. Optimal net thermoelectric power generation for four studied heat exchangers as function of occupancy ratio.

Optimized TEG is able to generate 137 MWh/year, taking into account that furnace works 8400 h a year, with power generation of 484.5 W/m^2 and average of 2.42 W/TEM. Produced electrical energy could supply 40 Spanish dwellings, just harvesting waste heat that furnace emits to the ambient with TEG formed by finned dissipators on hot side and thermosiphons on cold side.

5. Conclusions

Harvesting of waste heat to produce electrical energy via TEGs is a promising technology to help mitigate environmental issues that nowadays society is facing. TEGs are solid-state

systems, which barely present moving parts, and, therefore, they are very robust, reliable, silent and long-lasting.

Developed general computational model allows predicting behavior of any TEG. It does not include the most common simplifications that the rest of models from publications have and besides it includes new parameters, such as occupancy ratio, mass flow of refrigerants and temperature reduction in flue gases, while they flow along the system. The latter parameters are determinant for thermoelectric power generation and, therefore, very important to bear in mind for optimization study.

Thermal resistances of different heat exchange systems are function of novel parameter, occupancy ratio, included in computational model. Occupancy ratio has negative influence on thermal resistance per thermoelectric module, if it increases, due to the reduction in available dissipative area per TEM. Calorific power to dissipate influences just heat exchangers, where phase change is involved and mass flow of refrigerants determines thermal resistance, but in greater extent, when occupancy ratio has high values.

Thermosiphon with phase change is a dissipation system that provides the highest net thermoelectric power generation, 137 MWh/year, which is equivalent to supply 40 Spanish dwellings, when 32% of chimney surface is covered by TEMs. This production is 30, 72 and 87% higher than optimal productions of heat pipe, cold plate and finned dissipators, respectively. Moreover, the number of TEMs required for use in TEG with thermosiphons is lower or similar to that for the rest of heat dissipation systems, so not only power generation is optimum, but initial investment also.

The absence of moving parts for TEG built with thermosiphon procures really robust, reliable and silent power generation system that can produce electrical energy from waste heat of any system, improving their efficiency and, therefore, collaborating to satisfy demand for electrical energy in green manner.

Nomenclature

δ	Occupancy ratio
ϱ	Density, kg/m^3
σ	Thomson coefficient, V/K
α	Seebeck coefficient, V/K
π	Peltier coefficient, V
K	Thermal conductivity, W/(m × K)
c_p	Specific heat at constant pressure, J/(kg × K)
A_{TEM}	Area of a TEM, m^2
A_b	Area of the heat exchanger base, m^2
b_R^{TEM}	Systematic standard uncertainty
I	Current , A

http://dx.doi.org/10.5772/65849

I_{HP}	Current supplied to heat plates, A
M^{TEM}	Number of TEMs
M_{sample}	Number of samples for each configuration
$\dot{m}_{ai}$	Mass flow of air, kg/s
$\dot{m}_{gas}$	Mass flow of flue gases, kg/s
$\dot{m}_{w}$	Mass flow of water, kg/s
n_{blo}	Number of blocks of pipe
$\dot{Q}_{C}$	Heat power to dissipate, W
$\dot{Q}_{Joule}$	Joule heat power, W
$\dot{Q}_{Peltier}$	Peltier heat power, W
$\dot{Q}_{Thomson}$	Thomson heat power, W
$\dot{Q}^{i}$	Heat power extracted from flue gases in block "i", W
$\bar{q}$	Volumetric heat generation, W/m^3
R^{TEM}	Thermal resistance per thermoelectric module, K/W
R^{i}_{CD}	Thermal resistance of cold side heat dissipators of block "i", K/W
R^{i}_{cont}	Contact thermal resistance of block "i", K/W
R^{i}_{HD}	Thermal resistance of hot side heat dissipators of block "i", K/W
R^{i}_{per}	Thermal resistance of heat losses through free surface of block "i", K/W
R^{i}_{tor}	Thermal resistance of heat losses through bolts of block "i", K/W
R_0	Electrical resistance , Ohm
$s_{\bar{R}^{TEM}}$	Random standard uncertainty of the mean,
T_{amb}	Ambient temperature, K
T_C	Temperature of cold side , K
T_C^{TEMi}	Temperature of cold side of TEMs in block "i", K
T^{i}_{e}	Entry temperature of block "i", K
T^{i}_{H}	Temperature of heat source in block "i", K
T_H^{TEMi}	Temperature of hot side of TEMs in block "i", K

T_m^i	Mean temperature of block "i", K
T_m^{HX}	Mean temperature of heat exchanger, where heat is applied, K
T_s^i	Exit temperature of block "i", K
$U_{R^{TEM}}$	Expanded uncertainty
v_{gas}	Velocity of flue gases, m/s
V_{HP}	Voltage supplied to heat plates, V
$\dot{W}_{aux}$	Consumption of auxiliary equipment, W
$\dot{W}_{TEM}$	Thermoelectric power generation, W
$\dot{W}_{net}$	Net power generation, W

Author details

Patricia Aranguren[1,2*] and David Astrain[1,2]

*Address all correspondence to: patricia.arangureng@unavarra.es

1 Mechanical, Energy and Materials Engineering Department, Public University of Navarre, Pamplona, Spain

2 Smart Cities Institute, Pamplona, Spain

References

[1] Rattner AS, Garimella S. Energy harvesting, reuse and upgrade to reduce primary energy usage in the USA. Energy. 2011;36(10):6172–6183. doi:10.1016/j.energy.2011.07.047

[2] Torío H, Schmidt D. Development of system concepts for improving the performance of a waste heat district heating network with exergy analysis. Energy and Buildings. 2010;42(10):1601–1609. doi:10.1016/j.enbuild.2010.04.002

[3] Patil A, Ajah A, Herder P. Recycling industrial waste heat for sustainable district heating: A multi-actor perspective. International Journal of Environmental Technology and Management. 2009;10(3–4):412–426. doi:10.1504/IJETM.2009.023743

[4] Law R, Harvey A, Reay D. Opportunities for low-grade heat recovery in the UK food processing industry. Applied Thermal Engineering. 2013;53(2):188–196. doi:10.1016/j.applthermaleng.2012.03.024

[5] Rowe DM, Min G. Evaluation of thermoelectric modules for power generation. Journal of Power Sources. 1998;73(2):193–198. doi:10.1016/S0378-7753(97)02801-2

[6] Luo Q, Li P, Cai L, Zhou P, Tang D, Zhai P, et al. A thermoelectric waste-heat-recovery system for portland cement rotary kilns. Journal of Electronic Materials. 2014;44(6):1750–1762. doi:10.1007/s11664-014-3543-1

[7] Kuroki T, Murai R, Makino K, Nagano K, Kajihara T, Kaibe H, et al. Research and development for thermoelectric generation technology using waste heat from steelmaking process. Journal of Electronic Materials. 2015;44(6):2151–2156. doi:10.1007/s11664-015-3722-8

[8] Ma H, Lin C, Wu H, Peng C, Hsu C. Waste heat recovery using a thermoelectric power generation system in a biomass gasifier. Applied Thermal Engineering. 2015;88:274–279. doi:10.1016/j.applthermaleng.2014.09.070

[9] Aranguren P, Astrain D, Rodríguez A, Martínez A. Experimental investigation of the applicability of a thermoelectric generator to recover waste heat from a combustion chamber. Applied Energy. 2015;152:121–130. doi:10.1016/j.apenergy.2015.04.077

[10] Makki A, Omer S, Su Y, Sabir H. Numerical investigation of heat pipe-based photovoltaic-thermoelectric generator (HP-PV/TEG) hybrid system. Energy Conversion and Management. 2016;112:274–287. doi:10.1016/j.enconman.2015.12.069

[11] Ding LC, Akbarzadeh A, Date A. Transient model to predict the performance of thermoelectric generators coupled with solar pond. Energy. 2016;103:271–289. doi:10.1016/j.energy.2016.02.124

[12] Meng J-H, Wang X-D, Chen W-H. Performance investigation and design optimization of a thermoelectric generator applied in automobile exhaust waste heat recovery. Energy Conversion and Management. 2016;120:71–80. doi:10.1016/j.enconman.2016.04.080

[13] Tao C, Chen G, Mu Y, Liu L, Zhai P. Simulation and design of vehicle exhaust power generation systems: The interaction between the heat exchanger and the thermoelectric modules. Journal of Electronic Materials. 2015;44(6):1822–1833. doi:10.1007/s11664-014-3568-5

[14] Baker C, Vuppuluri P, Shi L, Hall M. Model of heat exchangers for waste heat recovery from diesel engine exhaust for thermoelectric power generation. Journal of Electronic Materials. 2012;41(6):1290–1297. doi:10.1007/s11664-012-1915-y

[15] Tritt TM. Thermoelectric phenomena, materials, and applications. Annual Review of Materials Research. 2011;41:433–448.

[16] Riffat SB, Ma X. Thermoelectrics: A review of present and potential applications. Applied Thermal Engineering. 2003;23(8):913–935. doi:10.1016/S1359-4311(03)00012-7

[17] Xie W, Tang X, Yan Y, Zhang Q, Tritt T. High thermoelectric performance BiSbTe alloy with unique low-dimensional structure. Journal of Applied Physics. 2009;105(11): 113713. doi:10.1063/1.3143104

[18] Heremans JP, Jovovic V, Toberer ES, Saramat A, Kurosaki K, Charoenphakdee A, et al. Enhancement of thermoelectric of the electronic density of states. Science. 2008;321 (July):1457–1461. doi:10.1126/science.1159725

[19] Culebras M, Gómez C, Cantarero A. Review on polymers for thermoelectric applications. Materials. 2014;6701–6732. doi:10.3390/ma7096701

[20] Kahraman F, Diez JC, Rasekh S, Madre MA, Torres MA, Sotelo A. The effect of environmental conditions on the mechanical and thermoelectric properties of $Bi_2Ca_2Co_{1.7}O_x$ textured rods. Ceramics International. 2015;41(5):6358–6363. doi:10.1016/j.ceramint.2015.01.070

[21] Zhang H, Wang Y, Dahal K, Mao J, Huang L, Zhang Q, et al. Thermoelectric properties of n-type half-Heusler compounds $(Hf_{0.25}Zr_{0.75})_{1-x}Nb_xNiSn$. Acta Materialia. 2016;113:41–47. doi:10.1016/j.actamat.2016.04.039

[22] Li X, Zhang Q, Kang Y, Chen C, Zhang L, Yu D, et al. High pressure synthesized Ca-filled $CoSb_3$ skutterudites with enhanced thermoelectric properties. Journal of Alloys and Compounds. 2016;677:61–65.doi:10.1016/j.jallcom.2016.03.239

[23] Chen J, Zuo L, Wu Y, Klein J. Modeling, experiments and optimization of an on-pipe thermoelectric generator. Energy Conversion and Management. 2016;122:298–309. doi: 10.1016/j.enconman.2016.05.087

[24] Yang Z, Winward E, Lan S, Stobart R. Optimization of the number of thermoelectric modules in a thermoelectric generator for a specific engine drive cycle. SAE Technical Papers. 2016. doi:10.4271/2016-01-0232

[25] Favarel C, Bédécarrats J-P, Kousksou T, Champier D. Experimental analysis with numerical comparison for different thermoelectric generators configurations. Energy Conversion and Management. 2015;107:114–122. doi:10.1016/j.enconman.2015.06.040

[26] Astrain D, Vián JG, Martínez A, Rodríguez A. Study of the influence of heat exchangers' thermal resistances on a thermoelectric generation system. Energy. 2010;35(2):602–610. doi:10.1016/j.energy.2009.10.031

[27] Martínez A, Vián JG, Astrain D, Rodríguez A, Berrio I. Optimization of the heat exchangers of a thermoelectric generation system. Journal of Electronic Materials. 2010;39(9):1463–1468. doi:10.1007/s11664-010-1291-4

[28] Wang XY, Wang SM, Zhou L, Li XC. Modeling and optimization of heat exchanger in automotive exhaust thermoelectric generator based on fluid kinematics. Advanced

Materials Research. 2014;9863–987:8483–851. doi:10.4028/www.scientific.net/AMR.986-987.848

[29] Su CQ, Wang WS, Liu X, Deng YD. Simulation and experimental study on thermal optimization of the heat exchanger for automotive exhaust-based thermoelectric generators. Case Studies in Thermal Engineering. 2014;4:85–91. doi:10.1016/j.csite.2014.06.002

[30] Barma MC, Riaz M, Saidur R, Long BD. Estimation of thermoelectric power generation by recovering waste heat from biomass fired thermal oil heater. Energy Conversion and Management. 2015;98:303–313. doi:10.1016/j.enconman.2015.03.103

[31] Wang CC, Hung CI, Chen WH. Design of heat sink for improving the performance of thermoelectric generator using two-stage optimization. Energy. 2012;39(1):236–245. doi:10.1016/j.energy.2012.01.025

[32] Esarte J, Min G, Rowe DM. Modelling heat exchangers for thermoelectric generators. Journal of Power Sources. 2001(Feb);93(1–2):72–76. doi:10.1016/S0378-7753(00)00566-8

[33] Amaral C, Brandão C, Sempels ÉV., Lesage FJ. Thermoelectric power enhancement by way of flow impedance for fixed thermal input conditions. Journal of Power Sources. 2014;272:672–680. doi:10.1016/j.jpowsour.2014.09.003

[34] Lesage FJ, Sempels ÉV., Lalande-Bertrand N. A study on heat transfer enhancement using flow channel inserts for thermoelectric power generation. Energy Conversion and Management. 2013;75:532–541. doi:10.1016/j.enconman.2013.07.002

[35] Zhou S, Sammakia BG, White B, Borgesen P, Chen C. Multiscale modeling of thermoelectric generators for conversion performance enhancement. International Journal of Heat and Mass Transfer. 2015;81:639–645. doi:10.1016/j.ijheatmasstransfer.2014.10.068

[36] Brito FP, Martins J, Hançer E, Antunes N, Gonçalves LM. Thermoelectric exhaust heat recovery with heat pipe-based thermal control. Journal of Electronic Materials. 2015;44(6):1984–1997. doi:10.1007/s11664-015-3638-3

[37] Jang J, Chi R, Rhi S, Lee K, Hwang H, Lee J, et al. Heat pipe-assisted thermoelectric power generation technology for waste heat recovery. Journal of Electronic Materials. 2015;44(6):2039–2047. doi:10.1007/s11664-015-3653-4

[38] Singh R, Tundee S, Akbarzadeh A. Electric power generation from solar pond using combined thermosyphon and thermoelectric modules. Solar Energy. 2011; 85(2):371–378. doi:10.1016/j.solener.2010.11.012

[39] Kim S, Park S, Kim S, Rhi SH. A thermoelectric generator using engine coolant for light-duty internal combustion Engine-Powered Vehicles. Journal of Electronic Materials. 2011;812–816. doi:10.1007/s11664-011-1580-6

[40] Aranguren P, Astrain D, Pérez MG. Computational and experimental study of a complete heat dissipation system using water as heat carrier placed on a thermoelectric generator. Energy. 2014;74(C):346–358. doi:10.1016/j.energy.2014.06.094

[41] Massaguer E, Massaguer A, Montoro L, Gonzalez JR. Development and validation of a new TRNSYS type for the simulation of thermoelectric generators. Applied Energy. 2014;134:65–74. doi:10.1016/j.apenergy.2014.08.010

[42] Meng JH, Zhang XX, Wang XD. Characteristics analysis and parametric study of a thermoelectric generator by considering variable material properties and heat losses. International Journal of Heat and Mass Transfer. 2015;80:227–235. doi:10.1016/j.ijheatmasstransfer.2014.09.023

[43] Montecucco A, Buckle JR, Knox AR. Solution to the 1-D unsteady heat conduction equation with internal Joule heat generation for thermoelectric devices. Applied Thermal Engineering. 2012;35(1):177–184. doi:10.1016/j.applthermaleng.2011.10.026

[44] Nguyen NQ, Pochiraju KV. Behavior of thermoelectric generators exposed to transient heat sources. Applied Thermal Engineering. 2013;51(1–2):1–9. doi:10.1016/j.applthermaleng.2012.08.050

[45] Meng F, Chen L, Sun F. A numerical model and comparative investigation of a thermoelectric generator with multi-irreversibilities. Energy. 2011;36(5):3513–3522. doi:10.1016/j.energy.2011.03.057

[46] Meng F, Chen L, Sun F. Effects of temperature dependence of thermoelectric properties on the power and efficiency of a multielement thermoelectric generator. International Journal of Energy and Environment. 2012;3(1):137–150.

[47] Lineykin S, Ben-Yaakov S. Modeling and analysis of thermoelectric modules. IEEE Transactions on Industry Applications. 2007;43(2):505–512. doi:10.1109/TIA.2006.889813

[48] Alata M, Al-Nimr MA, Naji M. Transient behavior of a thermoelectric device under the hyperbolic heat conduction model. International Journal of Thermophysics. 2003;24(6):1753–1768. doi:10.1023/B:IJOT.0000004103.26293.0c

[49] Rodríguez A, Vián JG, Astrain D, Martínez A. Study of thermoelectric systems applied to electric power generation. Energy Conversion and Management. 2009;50(5);1236–1243. doi:10.1016/j.enconman.2009.01.036

[50] Coleman HW, Steele WG. Experimentation, Validation, and Uncertainty Analysis for 25 Engineers, 3rd Edition. John Wiley & Sons, Inc., Hoboken, New Jersey.

[51] Aranguren P, Astrain D, Martínez A. Study of complete thermoelectric generator behavior including water-to-ambient heat dissipation on the cold side. Journal of Electronic Materials. 2014;43(6):2320–2330. doi:10.1007/s11664-014-3057-x

[52] TG12-8-01L Power Generators|Generator Modules. http://www.marlow.com/power-generators/standard-generators/tg12-8-01l.html